https://doi.org/10.5194/acp-2021-311
Preprint. Discussion started: 9 June 2021

Atmospheric Chemistry and Physics Discussions

Measurement report: Spatiotemporal and policy-related variations of $PM_{2.5}$ compositions and sources during 2015-2019 at multisite of a Chinese megacity

Xinyao Feng[1], Yingze Tian[1,2*], Qianqian Xue[1], Danlin Song[3], Fengxia Huang[3], and Yinchang Feng[1]

[1]State Environmental Protection Key Laboratory of Urban Ambient Air Particulate Matter Pollution Prevention and Control, College of Environmental Science and Engineering, Nankai University, Tianjin, 300071, China
[2]CMA-NKU Cooperative Laboratory for Atmospheric Environment-Health Research (CLAER/CMA-NKU)
[3]Chengdu Research Academy of Environmental Sciences, China

Correspondence to: Yingze Tian (tianyingze@hotmail.com; 015058@nankai.edu.cn)

Abstract. A thorough understanding of the relationship between urbanization and $PM_{2.5}$ (fine particulate matter with aerodynamic diameter less than 2.5 μm) variation is crucial for researchers and policymakers to study health effects and improve air quality. In this study, we selected a fast-developing Chinese megacity as the studied area to investigate the spatiotemporal and policy-related variations of $PM_{2.5}$ compositions and sources based on a long-term observation at multisite. A total of 836 samples were collected at 19 sites in wintertime of 2015-2019. According to the specific characteristics, 19 sampling sites were assigned into three layers. Layer 1 was the most urbanized area referred to the core zone of Chengdu, layer 2 was located in the outside circle of layer 1, and layer 3 belonged to the outer-most zone with the lowest urbanization level. The averaged $PM_{2.5}$ concentrations for five years were in the order of layer 2 (133 μg m^{-3}) > layer 1 (126 μg m^{-3}) > layer 3 (121μg m^{-3}). And for each year, the spatial clustering of chemical compositions at sampling sites was generally consistent with the classification of layers. $PM_{2.5}$ compositions for layer 3 in 2019 were found to be similar to that for other layers two or three years ago, implying that the urbanization levels had a strong effect on air quality. During the sampled period, a decreasing trend was observed for the annual averaged $PM_{2.5}$ concentrations, especially at sampling sites in layer 1, which was caused by the more strict control policies implemented in layer 1. The SO_4^{2-}/NO_3^- mass ratio at most sites exceeded 1 in 2015 but dropped less than 1 since 2016, reflecting decreasing coal combustion and increasing traffic impacts in Chengdu. The positive matrix factorization (PMF) model was applied to quantify $PM_{2.5}$ sources. A total of five sources were identified with the average contributions of 15.5% (traffic emission), 19.7% (coal and biomass combustion), 8.8% (industrial emission), 39.7% (secondary particles) and 16.2% (resuspended dust), respectively. From 2015 to 2019, dramatical decline was observed in the average percentage contributions of coal and biomass combustion, but traffic emission source showed an increasing trend. For spatial variations, coal and biomass combustion and industrial emission showed the stronger distribution patterns. High contributions of resuspended dust were occurred at sites with intensive construction activities such as subway and airport constructions. Combining the PMF results, we developed the source weighted potential source contribution function (SWPSCF) method for source localization, this new method highlighted the influences of spatial distribution for source contributions, and the effectiveness of the SWPSCF method was well-evaluated.

1 introduction

$PM_{2.5}$, fine particulate matter with aerodynamic diameter less than 2.5 μm, is a complex heterogeneous mixture of chemical constituents originating from a variety of sources (Bressi et al., 2013; He et al., 2019; Kelly and Fussell, 2012). Numerous epidemiological studies have reported associations between $PM_{2.5}$ and adverse human health effects (Bell Michelle et al., 2007; Yang et al., 2018b; Ostro et al., 2010; Philip et al., 2014), and attracted broad attention to $PM_{2.5}$ in public in the past decades. The link between urbanization and spatiotemporal variability of $PM_{2.5}$ has been studied (Zhang et al., 2015; Li et al., 2016). $PM_{2.5}$ generally presented an increasing trend along with urbanization (Yang et al., 2018a). In addition, multiple policies were

https://doi.org/10.5194/acp-2021-311
Preprint. Discussion started: 9 June 2021

Atmospheric Chemistry and Physics Discussions

conducted by governments to alleviate the pollution (Yan et al., 2018; Cai et al., 2017). The urbanization stage and emphasis of policies vary greatly in both time and space (Wang et al., 2018a; Gurjar et al., 2016; Seto et al., 2017), causing the significant spatiotemporal heterogeneity in the $PM_{2.5}$ distribution. Thus, a thorough understanding of the spatiotemporal and policy-related variations of $PM_{2.5}$ is necessary to investigate the relationship between urbanization and $PM_{2.5}$. Previous studies have investigated the spatiotemporal variability of $PM_{2.5}$ with the impact of urbanization (Li et al., 2016; Timmermans et al., 2017; Zhang et al., 2019; Yang et al., 2020; Seto et al., 2017), among which a small number of literatures devoted to the analysis of $PM_{2.5}$ compositions and sources (Lin et al., 2014; Yan et al., 2018). However, there is a lack of research on multisite and long-term sampling for $PM_{2.5}$ compositions over a city-size area (Dai et al., 2020; Xu et al., 2020a; Fang et al., 2020). Systematic measurement based on multisite and long-term observation can provide valuable data for the comprehensive understanding of $PM_{2.5}$ characteristics and variations. Related studies are critical for promulgating targeted control policies from the perspective of urbanization.

In a city-size area, there exist a large number of natural and anthropogenic emission sources, such as soil or road dust, vehicle exhaust, biomass combustion, sea salt, forest fires, and they have great spatiotemporal variations (Zhang et al., 2015; Zhang et al., 2013; Mirowsky et al., 2013; Yang et al., 2018b). It is essential to identify and apportion $PM_{2.5}$ sources for providing targeted control policies. To date, receptor models have been applied in a number of source apportionment studies of $PM_{2.5}$, including factor analysis models (like PCA-MLR, PMF, UNMIX, and ME2) and chemical mass balance (CMB) techniques (Shi et al., 2009; Choi et al., 2015; Hasheminassab et al., 2014; Liu et al., 2015). These receptor models have been proved to be the effective methods of identifying and apportioning sources. Furthermore, to identify the likely source regions for a receptor site, a number of trajectory statistical methods have been widely applied, including concentration field (CF), concentration weighted trajectory (CWT), potential source contribution function (PSCF) and so on (Chen et al., 2011; Gebhart et al., 2011; Riuttanen et al., 2013; Kulshrestha et al., 2009b). For PSCF method, due to the sources showed discrepant spatial distribution patterns over the studied region, when trajectories passed over the grid cell in which a source category showed high local contributions, the probability of potential contribution for this grid cell should be relatively high in theory, which have been ignored during traditional PSCF modelling. Thus, the source weighted PSCF (SWPSCF) method would be developed in this work which combines PMF with PSCF and takes account of the spatial distribution of contributions for each source category. The SWPSCF can be employed as a valuable tool to obtain more precise hint on potential source areas.

In China, megacities have experienced frequent air pollution events in response to rapid economic growth and urbanization (Li et al., 2016; Luo et al., 2018), which promoted governments to take various measures to improve air quality. Chengdu, one of typical megacities in China, can represent an illustrative example of urbanization in a metropolitan region. Since the implementation of policies such as the Air Pollution Prevention and Control Action Plan (APPCAP), Blue Sky Protection Campaign and the thirteenth Five-Year Plan (Cai et al., 2017), air quality prevention in Chengdu has achieved remarkable success, and it is helpful for researchers to explore the spatiotemporal and policy-related variations of $PM_{2.5}$. In this study, we investigated the spatiotemporal and policy-related variations of $PM_{2.5}$ compositions and sources in Chengdu at multisite based on a long-term observation. A total of 836 samples were collected in 19 sites of Chengdu in winters of 2015-2019. The positive matrix factorization (PMF) model was applied to estimate $PM_{2.5}$ source contributions. The SWPSCF method was applied to identify the potential source location. The main objectives of this study were: (i) to analyse the long-term spatiotemporal variations of $PM_{2.5}$ compositions among multiple zones in different urbanization levels; (ii) to determine $PM_{2.5}$ sources and their contributions, and to evaluate the effectiveness of the SWPSCF method in potential source localization; (iii) to explore the spatiotemporal evolution of sources along with changing of urbanization and related policy-orientation. The findings of this research will be helpful for a comprehensive understanding of the impact of urbanization process and control policy on variations of $PM_{2.5}$ compositions and sources in different zones, which can provide basic information for future

https://doi.org/10.5194/acp-2021-311
Preprint. Discussion started: 9 June 2021

Atmospheric Chemistry and Physics Discussions

epidemiological studies. And it is of vital importance for further formulating emission reduction policies in China and in other developing and polluting countries.

2 Method and materials

2.1 Sampling sites and sampling

We collected $PM_{2.5}$ samples in Chengdu (102° E to 104° E, 30° N to 31° N), which is in the southwest of China with a population of 16.33 million and the area of 14605 km^2. As the important metropolitan region in western China, Chengdu is undergoing rapid urbanization and is also attracting more and more people living here. At the same time, much attention was paid on the pollution of PM. To improve air quality, Chengdu government adopted several measures including limiting the driving area and time interval of highly polluted vehicles, adjusting industrial structures and implementing energy substitution. Considering the heterogeneous spatial distribution of population, economic, industry and construction activities, there exists great difference in urbanization and air quality in Chengdu, and emphasis on corresponding policies also varies over the city. As is shown in Fig. 1, the sampling was conducted at a total of 19 sites in Chengdu. Detailed information of sampling sites can be seen in Table S1. Based on the specific characteristics, 19 sampling sites were clustered in different zones for the convenience of discussion. Environment Protection Building (QY1), Chengdu University of Technology (CH1) and botanical garden (JN1) have similarities of high population density and high traffic. They are located in the core zone of Chengdu, and developed earlier in the urbanization process. Combining the city structure and evolution of urbanization level, Chengdu citizens are used to define regions surrounded by the third circle road as “layer 1”, and the location of QY1, CH1 and JN1 are in accordance with the extent of layer 1. Sampling sites including Qingbaijiang (QBJ2), Xindu (XD2), Pidu (PD2), Wenjiang (WJ2), Shuangliu (SL2), Tianfu (TF2) and Longquanyi (LQY2) are located in the outside circle of layer 1. The circle developed later than layer 1 and were clustered as the second zone named as layer 2. Among the sampling sites in layer 2, QBJ2, XD2, WJ2 and SL2 are featured by intensive industrial factories, and TF2 has frequent construction activities. The remaining 9 sites (Jintang (JT3), Pengzhou (PZ3), Dujiangyan (DJY3), Chongzhou (CZ3), Dayi (DY3), Qionglai (QL3), Pujiang (PJ3), Xinjin (XJ3) and Jianyang (JY3)) are located in the outer-most zone of Chengdu, which belongs to layer 3. The urbanization level of layer 3 is lower than layer 1 and layer 2. In addition, because the air pollution is usually heavy in winter, the sampling campaign was conducted in winter from 2015 to 2019, lasting about 15 days each year. The detailed sampling periods for sampling sites in 2015-2019 are listed in Table S2. Although several selected sampling sites may not fully consistent in each year, this small difference will not influence the reflection of spatiotemporal variations in Chengdu. A total of 836 $PM_{2.5}$ samples were collected for analysis.

The sampling campaign was conducted by two medium-volume air samplers (TH-150C; Wuhan Tianhong Ltd., China) with the airflow rate of 100 min L^{-1} were used at each site. One sampler placed quartz filters to collect $PM_{2.5}$ for analysing organic (OC), elemental carbon (EC) and ions. The other sampler placed polypropylene filters for analysing elements in $PM_{2.5}$. $PM_{2.5}$ samples were daily collected for 22h at 19 sites. Information of average temperature (℃), cumulative volume (L) and standard volume (L) were recorded. Collected samples were stored in a layer of aluminium foil in a freezer at -20℃ until weighing and analysis. The mass of $PM_{2.5}$ was determined by weight difference of the filter before and after sampling. Before sampling, blank quartz filters and blank polypropylene filters were baked at 600 ℃ for 4h and 60 ℃ for 3h, respectively. For the process of weighing, filters were weighted at a temperature of 20±1℃ and a humidity of 40±5% for 48h. The weights of filters can be obtained using a microbalance with a sensitivity level of 0.01 mg. Each filter was weighted twice, and the final weight equals to the average of two values (the difference was less than 0.05 mg).

https://doi.org/10.5194/acp-2021-311
Preprint. Discussion started: 9 June 2021

Atmospheric Chemistry and Physics Discussions

2.2 Chemical analysis and quality assurance/ quality control (QA/QC)

The OC, EC, ions and elements were detected by the thermal/optical carbon aerosol analyser (DRI model 2001A; Desert Research Institute, USA), ion chromatograph system (ICS-900; DIONEX, USA) and Inductively Coupled Plasma Atomic Emission Spectrometer (ICAP 7400 ICP-AES; Thermo Fisher Scientific, USA), respectively.

OC and EC were analysed based on a hole with 0.588 cm^2 of the quartz filter. The thermal/optical carbon aerosol analyser orderly detected OC1, OC2, OC3 and OC4 in a pure helium atmosphere at the temperature of 140℃, 280℃, 480℃, and 580℃, respectively. Likewise, the oven increased the temperature to 540℃, 780℃, and 840℃ for EC1, EC2 and EC3 analysis, respectively, in a 2% O_2 atmosphere. The organic pyrolyzed carbon (OPC) would also be detected after adding the oxygen. Finally, the OC and EC concentrations were calculated as Eq. (1) and Eq. (2), respectively. QA/QC was conducted by the calibration process. The analyser will be calibrated before and after analysing to make sure the analytic accuracy within 2%.

$$OC = OC_1 + OC_2 + OC_3 + OC_4 + OPC \quad (1)$$

$$EC = EC_1 + EC_2 + EC_3 - OPC \quad (2)$$

Ions such as Cl^-, SO_4^{2-}, NO_3^- and NH_4^+ were measured on a one-eighth sample. Samples were cut up into small pieces and ultrasonically extracted with 8mL deionized water for 20 minutes. Tubes that were used during extracting had been cleaned three times by an ultrasonic cleaner. After extracting, the supernatant was injected into a vial through two 0.22μm filters for analysis. Relative standard deviations had to be calculated more than three times to hold the value at a lower level.

As for elements analysis, the microwave acid digestion method was applied for detecting Al, Fe, Mg, Ca, Na, K, V, Cd, Pb, Si, Zn, Cu, Cr, As, Ni, Co, Mn and Ti. 10mL mixed digestion solution was added to digest one-eighth sample pieces, the digestion process was conducted by four-stage microwave digestion procedure of the microwave-accelerated reaction system (MARS; CEM Corporation, USA). Afterward, the digestion solution would be transferred into a PET bottle, and diluted the solution to 25ml by deionized water for further analysis.

2.3 Positive Matrix Factorization (PMF)

The PMF model is a widely used bilinear receptor model. The goal of this model is to identify and quantify the source contribution of contaminants by solving the following equation (Eq. (3)):

$$x_{ij} = \sum_{k=1}^{p} g_{ik} f_{kj} + e_{ij} \quad (3)$$

where i, j and p are the number of samples, chemical compositions, and factors, respectively; x_{ij} is the concentration of the j_{th} species in the i_{th} sample; g_{ik} is the contribution of the k_{th} source to the i_{th} sample; f_{kj} is the concentration of the j_{th} species from the k_{th} source; and e_{ij} is the residual for each sample/species (Paatero, 1997; Paatero and Tapper, 1994).

We input the measured speciated data as the matrix X of i by j dimensions, then the PMF model can divide it into two matrixes: factor contributions (G) and factor profiles (F). The non-negativity constraint is also introduced to ensure the positive value for each source contribution. In the process of decomposition, the model is run several times applying the least square method to minimize the objective function Q (Eq. (4)), and in this case, the obtained solution of G and F is considered the most optimal:

$$Q = \sum_{i=1}^{n} \sum_{j=1}^{m} \left(\frac{e_{ij}}{u_{ij}}\right)^2 \quad (4)$$

where u_{ij} is the uncertainty of the j_{th} chemical composition of the i_{th} sample. The model required both concentration data and uncertainty of species in each sample. The equation-based uncertainty is calculated as follows (Eq. (5)):

https://doi.org/10.5194/acp-2021-311
Preprint. Discussion started: 9 June 2021

Atmospheric Chemistry and Physics Discussions

$$u_{ij}=\begin{cases}\frac{5}{6}\times MDL, & c_{ij}\le MDL\\ \sqrt{\left(Error\ Fraction\times c_{ij}\right)^2+(0.5\times MDL)^2}, & c_{ij}>MDL\end{cases} \quad (5)$$

where c_{ij} is the concentration of chemical compositions of each sample, MDL is the method detection limit for each component.

In this study, the EPA PMF 5.0 was applied for the source apportionment of $PM_{2.5}$, and total of 22 chemical compositions of 836 samples at 19 sites from 2015 to 2019 were simulated. The detailed source apportionment results are reported in 3.3 and more information on the PMF model is described in the PMF 5.0 User Guide.

2.4 Source Weighted Potential Source Contribution Function (SWPSCF)

The PSCF model is a conditional probability that was applied to identify the source regions of $PM_{2.5}$ masses to the receptor site. In this study, the backward trajectories were modelled by the hybrid single-particle Lagrangian Integrated Trajectory (HYSPLIT 4.9 version), which is available at http://www.arl.noaa.gov/ready/hysplit4.html. Required meteorological data can be obtained from National Oceanic and Atmospheric Administration (NOAA) website (ftp://arlftp.arlhq.noaa.gov/pub/archives/reanalysis). The 12 h backward trajectories starting from the receptor site at 500 m above ground level were generated with 6 h time intervals during all sampling periods. PSCF model divided the region where trajectories passed over into 0.1°×0.1° grid cells and computed PSCF values of all grid cells in the domain. For the receptor site, the daily concentrations were assigned to the grid cells along related trajectories, and selected a certain threshold criteria value. When the concentration in one grid cell was above the threshold value, there exists a probability that sources located in this grid cell has an influence on the receptor $PM_{2.5}$ concentrations. A higher PSCF value indicates a higher probability of this. The PSCF values were defined by Eq. (6) (Han et al., 2007):

$$PSCF_{ij}=\left(\frac{m_{ij}}{n_{ij}}\right)W_{ij} \quad (6)$$

where n_{ij} is the total number of trajectory endpoints that fall into the grid cell (i, j), and m_{ij} is the number of trajectory endpoints when their corresponding contributions exceed the criteria value. W_{ij} is a weight function (Eq. (7)) used for reducing uncertainty when specific grid cells have small numbers of trajectory endpoints (Polissar et al., 2001; Lee and Hopke, 2006):

$$W_{ij}=\begin{cases}1.0 & 3n_{ave}<n_{ij}\\ 0.7 & 1.5n_{ave}<n_{ij}<3n_{ave}\\ 0.4 & n_{ave}<n_{ij}<1.5n_{ave}\\ 0.2 & n_{ij}<n_{ave}\end{cases} \quad (7)$$

where n_{ave} is the average number of endpoints in each grid cell.

When trajectories passed over a grid cell in which a certain source category showed high local contribution, the probability of potential contribution for this grid cell should be relatively high. Thus, we introduced another weighted function SW_{ij} that represents the ratio of source contribution in grid cell (i, j) to average contribution in the whole study area. The SW_{ij} is calculated as Eq. (8). The source weighted PSCF (SWPSCF) value is expressed as Eq. (9).

$$SW_{ij}=c_{ij}/c_{ave} \quad (8)$$

$$SWPSCF=SW_{ij}\times PSCF \quad (9)$$

where c_{ij} is the source contribution of each source category in grid cell (i, j), and is available using the Kriging interpolation algorithm; c_{ave} is the average source contribution of this source category of all sampling sites in the whole study area.

https://doi.org/10.5194/acp-2021-311
Preprint. Discussion started: 9 June 2021

Atmospheric Chemistry and Physics Discussions

2.5 Hierarchical cluster analysis (HCA)

The similarity analysis of $PM_{2.5}$ compositions among the 19 sampling sites from 2015 to 2019 was conducted using the method of hierarchical cluster analysis. Cluster analysis, a technique used for identifying groups that have similar characteristics, can be broadly classified as hierarchical and non-hierarchical (Govender and Sivakumar, 2020; Saxena et al., 2017). By recursively finding nested clusters, hierarchical clustering repeatedly combines the two closest groups into one larger group (Xu et al., 2020b), and finally generates a dendrogram. The algorithm is implemented mainly by the following steps (Govender and Sivakumar, 2020):

Step 1: Determine each observation as the initial cluster.

Step 2: Measure the distance between clusters for quantifying the similarity between objects.

Step 3: The closest pairs of clusters are merged into a single cluster, and re-calculate the distance matrix.

Step 4: Repeat step 2 and 3 until all observations are integrated into a single cluster.

In this study, the HCA was conducted based on the cosine distance and average linkage using IBM SPSS Statistics 25. By cutting the dendrogram at an appropriate distance, $PM_{2.5}$ samples that have similarities in chemical species can be grouped into the same cluster.

3 Results and discussion

3.1 Spatiotemporal variations of $PM_{2.5}$ concentrations

The spatiotemporal variations of $PM_{2.5}$ concentrations for layers and sites in 2015-2019 are depicted in Fig. 2. And the detailed $PM_{2.5}$ concentrations are summarized in Table S3. Due to the slight difference of the selected sampling sites in layer 2 and layer 3 in each year, both layers and sites were discussed for a better understanding of the $PM_{2.5}$ variability. For spatial distribution, the average $PM_{2.5}$ concentrations of five years were 126 μg m^{-3}, 133 μg m^{-3} and 121 μg m^{-3} for layer 1, layer 2 and layer 3, respectively. Layer 1, the most urbanized area in Chengdu, suffered severe traffic pollution, however, more strict control policies were conducted by local government in this area. The high $PM_{2.5}$ concentration in layer 2 may be caused by strong industrial activities and extensive construction activities at QBJ2, XD2, WJ2, SL2 and TF2. Layer 3 was characterized by the lowest urbanization level in Chengdu, although weak emissions of old chemical industries and small coal-fired boilers were observed at XJ3, PZ3, CZ3 and DY3, there existed less vehicles than layer 1 and less factories than layer 2, explaining the relatively low $PM_{2.5}$ level of the area.

$PM_{2.5}$ concentrations in three layers showed similar temporal variation, which averagely declined from 174 μg m^{-3} in 2015 to 95 μg m^{-3} in 2019, except for a small increase in 2017 (134 μg m^{-3}), indicating the effective control measures in Chengdu in recent years. A more obvious decline was observed at sites in layer 1. In 2015, $PM_{2.5}$ concentration was the highest in layer 1, however since 2016, the highest $PM_{2.5}$ level have transferred from layer 1 to layer 2. This may be influenced by the fact that the coal-burning ban was promulgated the earliest in layer 1. The government published Chengdu's Air Pollution Prevention and Control Regulation in each year and introduced a number of specific measures, among which the substitution of the clean energy boilers for existing coal-fired boilers was accelerated in 2016 in layer 1. $PM_{2.5}$ concentrations at several sites in layer 2 exhibited a minor elevation: for example, $PM_{2.5}$ levels at WJ2 and SL2 elevated in 2018. It may be associated with the construction and industrial activities in this region. Temporal variations of sites in layer 3 are not discussed due to the deficiency of $PM_{2.5}$ concentrations in many studied years.

3.2 Spatiotemporal variations of chemical compositions

Research in chemical compositions of $PM_{2.5}$ can be helpful to identify the source changes and the effectiveness of related

https://doi.org/10.5194/acp-2021-311
Preprint. Discussion started: 9 June 2021

Atmospheric Chemistry and Physics Discussions

policies. Figure 3 shows the fractions of main chemical species (%) in $PM_{2.5}$ at each site during winters in 2015-2019, reflecting the relative importance of species under different $PM_{2.5}$ concentrations. The average fractions of $PM_{2.5}$ species were in the order of OC > NO_3^- > SO_4^{2-} > crustal elements (the sum of Al, Si, Ca, Ti and Fe) > NH_4^+ > EC > Cl^-, constituting 17.2%, 13.5%, 11.0%, 8.3%, 5.7%, 5.4%, 2.3% of the $PM_{2.5}$ mass, respectively.

To identify the similarity and diversity of $PM_{2.5}$ compositions among the sampling sites and years, Figure 4 describes the hierarchical cluster analysis (HCA) results (based on cosine distances) of chemical compositions (%) at each sampling site for five years (2015-2019). Four clusters were revealed, and the result showed a strong correlation with years: cluster 1 (C1) included all the sites in 2015; sites in 2016 and 2017 were classified as cluster 2 (C2); cluster 3 (C3) consisted of most sites in 2018 and 2019; and 2016DJY3, the only sites far from the other sites, was separated as cluster 4 (C4) due to its distinctive pollution feature. The meteorological data during the sampling period from 2015 to 2019 is shown in Table S4, reflecting the similar meteorological conditions in the studied years, which highlighted the importance of the source variations for the clustering result. There existed a special case that sites of layer 3 in 2019 belonged to C2 rather than C3, indicating $PM_{2.5}$ compositions for layer 3 in 2019 were more similar to that for other layers two or three years ago. This can be explained by the fact that the urbanization levels varied between layers in Chengdu. As the outer-most zone of Chengdu, layer 3 lagged behind layer 1 and layer 2 in the urbanization, which contributed to the similar characteristics in air quality between current layer 3 and previous other layers. The HCA results indicated an incredible need to investigate the variations of $PM_{2.5}$ compositions in both time and space.

3.2.1 Spatial variations of chemical compositions

To investigate the spatial similarities and differences of chemical compositions, the HCA was also applied based on chemical compositions (%) at sampling sites for each year, and finally cluster results and their averaged species fractions are listed in Fig. S1. It's interesting to find that the spatial clustering in each year was generally consistent with the classification of three layers. For example, sites in Layer 3 were generally clustered in specific clusters.

The chemical compositions of clusters in 2015-2019 are shown in Fig. 5. Take an example of the first cluster in 2015, we defined it as 2015C1. Spatial differences were observed for each year. Clusters containing sites in layer 3 (2015C4, 2016C4, 2017C1, 2018C2 and 2019C1) always showed higher OC fractions which were 20.9%, 14.6%, 20.5%, 17.5% and 23.3% of $PM_{2.5}$ mass, respectively. The higher OC fractions in layer 3 may indicate stronger fuel combustion and biomass burning. One possible reason was that there were more residential combustions (like bulk coal and biofuel combustions) and small boilers with low combustion efficiency in layer 3 than in the other two layers, so control measures for fuel combustion is still needed to be strengthened in layer 3. The high NO_3^- level in Chengdu were observed at PZ3 in 2015 and QY1, CH1 in 2019. The high NO_3^- level at PZ3 in 2015 may be associated with the petrochemistry industry. In 2019, the NO_3^- level at PZ3 was lower than that in 2015, which might be influenced by the renovation of de-nitrification of the key industries. On the other hand, the vehicle ownership in Chengdu markedly increased especially in layer 1. Characterized by the most intensive vehicles, QY1 and CH1 was observed to suffer traffic pollution. Crustal elements accounted for the highest proportion in layer 1 related clusters (2016C3, 2017C3 and 2018C4) with 10.5%, 9.9% and 8.3%, respectively. The subway construction of in layer 1 of Chengdu can explain this result well.

3.2.2 Temporal variations of chemical compositions

For temporal variations of compositions shown in Fig. 3, the fractions of OC and EC generally showed a decreasing trend from 2015 to 2018 and slightly increased in 2019 at most sites. The average fractions of OC were 19.1% and 15.5% in 2015 and 2018, respectively. EC accounted for 15.5% and 5.0% of $PM_{2.5}$ in 2015 and 2018, respectively. The OC and EC mainly

https://doi.org/10.5194/acp-2021-311
Preprint. Discussion started: 9 June 2021

Atmospheric Chemistry and Physics Discussions

come from fuel combustion, such as coal, gasoline, diesel, biomass, and so on (Wang et al., 2020). In Chengdu, coal is one of the important fuels for the industry but has been strongly reduced by the government in recent years. Gasoline and diesel are mainly used for vehicles. The decrease of OC and EC fractions from 2015 to 2018 may due to the decline of coal use for industries, which was consistent with the strict coal-burning ban in these years, however, as the vehicles become more important contributor, the OC and EC fractions increased in 2019. Publications have reported the SO_4^{2-} and Cl^- as the coal-burning markers (Tian et al., 2014; Vassura et al., 2014). In this study, the fractions of SO_4^{2-} and Cl^- generally showed a decreasing trend, especially in 2016. However, the fractions of NO_3^- showed a general increasing trend from 2015 to 2019, which might be attributed to the gradually enhanced contribution of vehicles and use of natural gas. We also analyzed the SO_4^{2-} /NO_3^- mass ratio, a qualitative indicator of sulfur versus nitrogen sources (Gao et al., 2015; Arimoto et al., 1996), and the summary is listed in Fig. S2. Ratios at most sites exceeded 1 in 2015, dropped less than 1 in 2016 and then declined steadily, also indicating decreasing coal combustion and increasing traffic emissions in Chengdu. The result was consistent with the slow reduction in NO_X and the sharp decline in SO_2 emissions in China (Zhao et al., 2013; Wang et al., 2018b). For crustal elements, the temporal variations were found to have close relationship with the construction activities in Chengdu in 2015-2019.

3.3 Spatiotemporal variations of sources

PMF was used to quantify the source contributions in the studied areas and finally five categories were selected with distinctively related source characteristics. Five sources were identified as traffic emission, coal and biomass combustion, industrial emission, secondary particles and resuspended dust, respectively. The estimated source profiles in the form of species concentrations (μg m^{-3}) and percentages of species sum (%) are shown in Fig. 6. Factor 1 contributed 15.5% of $PM_{2.5}$ and had high fractions of EC (70.0% of total EC) and OC (51.8% of total OC), which can be identified as traffic emission (Xu et al., 2016). The relatively high NO_3^- further revealed factor 1 as the traffic emission source. The moderate fractions of Al, Si, Cu, Ni and As in this factor may be associated with traffic activities including resuspension of road dust, tire and brake wear, and oil burning (Kulshrestha et al., 2009a; Almeida et al., 2005; Amato and Hopke, 2012). Factor 2 was determined as coal and biomass combustion source. Coal combustion generally plays an important role in Chinese energy structure. Identified as markers of coal combustion source, OC, EC, Cd and SO_4^{2-} exhibited high loadings in factor 2, with fractions of 25.8%, 20.3%, 61.9% and 26.7%, respectively (Tian et al., 2016). The existence of biomass burning was indicated by the high fraction of K^+ in this factor (Amil et al., 2016; Richard et al., 2011). Factor 2 accounted for 19.7% of the total $PM_{2.5}$ mass concentration. Factor 3, which accounted for 8.8% of $PM_{2.5}$, was considered as an industrial emission source, due to its high loadings of Fe (73.8%), Cu (70.7%), Mn (60.5%), Ti (85.5%), Ni (61.5%) and Mg (50.2%). The above species are used frequently as source markers for industrial emissions including building materials and metallurgical production (Contini et al., 2014; Jiang et al., 2014). Factor 4 was characterized by nearly 76.7%, 61.2% and 55.9% of NO_3^-, NH_4^+ and SO_4^{2-}, and no other high species. According to previous studies, NO_3^-, SO_4^{2-} and NH_4^+ are indicative species of secondary reactions (Richard et al., 2011; Wu et al., 2021). Consequently, factor 4 represented the secondary particle source, contributing 39.7% of $PM_{2.5}$. Factor 5 was identified as resuspended dust accounting for 16.2% of $PM_{2.5}$. The top three fractions of species were Al (84.2%), Ca (79.5%) and Si (56.5%), which were typical indicatory components for resuspended dust (Pant and Harrison, 2012).

3.3.1 Spatial variations of source contributions

Figure 7 shows the source contribution at each site from 2015 to 2019 to investigate their spatial variations. The CV (Coefficient of Variation), which is defined as the standard deviation divided by the mean, was used to investigate the spatial difference of each source category. As shown in Table S5, CV values in this study indicate that coal and biomass combustion and industrial emission showed stronger spatial variations. For coal and biomass combustion source, the percentage contributions were higher at CZ3 of layer 3 and QBJ2 of layer 2 than at other sites. And the high contributions of industry

https://doi.org/10.5194/acp-2021-311
Preprint. Discussion started: 9 June 2021


Atmospheric Chemistry and Physics Discussions

source mainly occurred in layer 2 including QBJ2, WJ2, PD2, SL2 and XD2, with fractions from 8.9% to 12.9%. Among the sampling sites mentioned above, CZ3 was characterized by intensive coal-fired boilers. QBJ2 contains large-scale iron, steel and chemical plants. WJ2, PD2, SL2 and XD2 were in great development and also had large factories of glass, food and furniture, respectively. Therefore, the spatial distributions of $PM_{2.5}$ from coal and biomass combustion and industrial emission were strongly associated with industrial manufacturing plants. Additionally, the contributions of traffic emission were higher in layer 1 and layer 2, with the percentage contributions in 2015-2019 ranging from 13.9% to 16.3% in layer 1 and from 11.6% to 17.5% in layer 2. The secondary particles had higher contributions in layer 3. Fractions of secondary particles at QY1 and LQY2 also presented relatively high values of 44.5% and 49.9%, respectively. For resuspended dust, the spatial distribution varied with human activities. The contributions were relatively higher at layer 1 in 2015-2018, which resulted from the construction of the urban subway. At JY3, high contributions from resuspended dust were attributed to the fact that Chengdu Tianfu International Airport was under construction. Overall, the spatial distributions of source contributions were exactly in accordance with the characteristics and urbanization level of sites, highlighting the importance of site-specific and urbanization research in pollutant emissions control.

To better consider the spatial distribution of contributions for each source category, the SWPSCF method was applied for identifying the source regions to the receptor site based on a source contribution weight. In this study, we selected QY1 as the receptor site and the averaged contribution of each source category at QY1 as threshold values. Both SWPSCF and PSCF values were calculated for each source category in the wintertime from 2015 to 2019. The effectiveness of the SWPSCF method was well-evaluated during the investigation. The examples of traffic emission and coal and biomass combustion in 2015 and 2019 were shown in Fig. 8, and differences were found in PSCF and SWPSCF results. For coal and biomass combustion source in 2015 (Fig. 8(a)), the potential source regions were observed to concentrate to CZ3 after source weighted, and the SWPSCF values around QBJ2 were higher than PSCF values, reflecting a strengthened influence of coal and biomass combustion source at CZ3 and QBJ2. For traffic emission source in 2019 (Fig. 8(b)), the identified potential source regions moved toward layer 1 after source weighted, which was in agreement with the spatial distribution of traffic emission contributions.

3.3.2 Temporal variations of source contributions

Temporal variations of source contributions at each site are also summarized in Fig. 7. Contributions of traffic emissions at most sites showed an increasing trend from 2015 to 2019, because the number of vehicles was fast increasing. The average percentage contributions of traffic emissions of layer 1 and layer 2 were in the order of 13.3% (in 2015) < 13.4% (in 2016) < 14.8% (in 2017) < 15.8% (in 2018) < 17.1% (in 2019). Contributions in layer 3 was not calculated because of the difference of sites in the studied year, but the tendency was consistent with conclusions of layer 1 and layer 2. An obvious decline in the contribution of coal and biomass combustion can be observed in studied years, especially in 2016. The average percentages of layer 1 and layer 2 declined from 33.2% in 2015 to 15.5% in 2016 and finally to 11.5% in 2019. The result indicated that notable success was achieved in the control of and coal-related sources in recent years. The industrial emission showed the highest percentages in 2016 at some sites and presented a downtrend. The percentage of source contributions of secondary particles at most sites increased steadily year by year. The average fractions of layer 1 and layer 2 from 2015 to 2019 were 29.8%, 40.0%, 41.2%, 46.0% and 44.0%, respectively. For resuspended dust, the fractions in 2015 and 2016 were generally higher than those in other years, especially for sites in layer 1 where had strong subway construction activities in previous years. In 2017-2019, the source contributions of resuspended dust remained stable, and some slight fluctuations can be attributed to local construction activities.

The above analysis of temporal variations provides insights on the changes of source structures in Chengdu: pollution from traffic and secondary aerosol were playing more important role; sources from coal and biomass combustion and industrial

https://doi.org/10.5194/acp-2021-311
Preprint. Discussion started: 9 June 2021


Atmospheric Chemistry and Physics Discussions

emissions were effectively controlled; and resuspended dust always happened along with the urban construction. All of the information can offer useful references for the government to furtherly promulgate effective policies on atmospheric pollution prevention and reduction in China and other developing and polluting countries.

4 Conclusion

We investigated the spatiotemporal and policy-related variations of $PM_{2.5}$ compositions and sources at 19 sites in Chengdu, based on a long-term sampling campaign in wintertime from 2015 to 2019. Considering the specific characteristics among sites, the variations were discussed in three layers that are in different urbanization levels. The results showed distinct spatiotemporal distribution patterns for both $PM_{2.5}$ compositions and sources, linking with the process of urbanization and corresponding policies in the studied region.

During the sampling period, temporal variations of averaged $PM_{2.5}$ concentrations at sites in layer 1 showed the most obvious decreasing trend, which was caused by comparably strict control measures conducted in layer 1. The fractions of OC and EC declined from 2015 to 2018 and slightly increased in 2019 at most sites. The SO_4^{2-}/NO_3^- mass ratio at most sites dropped less than 1 since 2016 and showed a decreasing trend, indicating decreasing coal combustion and increasing traffic emissions in Chengdu. The average percentage contributions of coal and biomass combustion source declined obviously from 2015 to 2019, reflecting the notable success in the control of coal-related sources in Chengdu. For spatial variations, $PM_{2.5}$ compositions for layer 3 in 2019 were found to be similar to that for layers two or three years ago, which indicated the great impact of differences in urbanization to air quality. Coal and biomass combustion and industrial emission showed the stronger spatial distribution patterns in Chengdu, the high percentage contributions of which usually occurred at sites with large-scale industrial factories and coal-fired boilers. Frequent construction activities in developing areas can considerably elevate the percentage contributions of resuspended dust. The SWPSCF results were found to have great differences with PSCF results. The changes for identified potential source regions after source weighted were in agreement with the spatial distribution of each source contributions. This study presented a perspective on the relationship between $PM_{2.5}$ and urbanization. Sampling activities that conducted based on a five-year measurement at 19 sites in different urbanization levels provided particular valuable data for researchers. The results can be useful for further policy formulation in most developing and polluted countries, and supply basic information for future epidemiological studies.

Data availability. The hybrid single-particle Lagrangian Integrated Trajectory (HYSPLIT 4.9 version) is available at http://www.arl.noaa.gov/ready/hysplit4.html (last access February 28th, 2021). Required meteorological data during SWPSCF modelling can be obtained from National Oceanic and Atmospheric Administration (NOAA) website, ftp://arlftp.arlhq.noaa.gov/pub/archives/reanalysis (last access February 28th, 2021).

Acknowledgments. This study is supported by the National Natural Science Foundation of China (41977181).

Author contributions. Xinyao Feng were responsible for the writing of the paper and performing the SWPSCF model; Yingze Tian provided the scientific idea and performed PMF experiments; Danlin Song and Fengxia Huang provided sampling data for analysis; Yingze Tian, Qianqian Xue and Yinchang Feng contributed to the project coordination.

Competing interests. The authors declare that they have no conflict of interest.

https://doi.org/10.5194/acp-2021-311
Preprint. Discussion started: 9 June 2021

Atmospheric Chemistry and Physics Discussions

References

Almeida, S. M., Pio, C. A., Freitas, M. C., Reis, M. A., and Trancoso, M. A.: Source apportionment of fine and coarse particulate matter in a sub-urban area at the Western European Coast, Atmospheric Environment, 39, 3127-3138, https://doi.org/10.1016/j.atmosenv.2005.01.048, 2005.

Amato, F. and Hopke, P. K.: Source apportionment of the ambient PM2.5 across St. Louis using constrained positive matrix factorization, Atmospheric Environment, 46, 329-337, https://doi.org/10.1016/j.atmosenv.2011.09.062, 2012.

Amil, N., Latif, M. T., Khan, M. F., and Mohamad, M.: Seasonal variability of PM2.5 composition and sources in the Klang Valley urban-industrial environment, Atmos. Chem. Phys., 16, 5357-5381, doi:10.5194/acp-16-5357-2016, 2016.

Arimoto, R., Duce, R. A., Savoie, D. L., Prospero, J. M., Talbot, R., Cullen, J. D., Tomza, U., Lewis, N. F., and Ray, B. J.: Relationships among aerosol constituents from Asia and the North Pacific during PEM-West a, Journal of Geophysical Research Atmospheres, 101, 2011-2023, doi:10.1029/95JD01071, 1996.

Bell Michelle, L., Dominici, F., Ebisu, K., Zeger Scott, L., and Samet Jonathan, M.: Spatial and Temporal Variation in PM2.5 Chemical Composition in the United States for Health Effects Studies, Environmental Health Perspectives, 115, 989-995, doi:10.1289/ehp.9621, 2007.

Bressi, M., Sciare, J., Ghersi, V., Bonnaire, N., Nicolas, J. B., Petit, J. E., Moukhtar, S., Rosso, A., Mihalopoulos, N., and Féron, A.: A one-year comprehensive chemical characterisation of fine aerosol (PM2.5) at urban, suburban and rural background sites in the region of Paris (France), Atmos. Chem. Phys., 13, 7825-7844, doi:10.5194/acp-13-7825-2013, 2013.

Cai, S., Wang, Y., Zhao, B., Wang, S., Chang, X., and Hao, J.: The impact of the "Air Pollution Prevention and Control Action Plan" on PM2.5 concentrations in Jing-Jin-Ji region during 2012–2020, Science of The Total Environment, 580, 197-209, https://doi.org/10.1016/j.scitotenv.2016.11.188, 2017.

Chen, L. W. A., Watson, J. G., Chow, J. C., DuBois, D. W., and Herschberger, L.: PM2.5 Source Apportionment: Reconciling Receptor Models for U.S. Nonurban and Urban Long-Term Networks, Journal of the Air & Waste Management Association, 61, 1204-1217, doi:10.1080/10473289.2011.619082, 2011.

Choi, J.-K., Ban, S.-J., Kim, Y.-P., Kim, Y.-H., Yi, S.-M., and Zoh, K.-D.: Molecular marker characterization and source appointment of particulate matter and its organic aerosols, Chemosphere, 134, 482-491, https://doi.org/10.1016/j.chemosphere.2015.04.093, 2015.

Contini, D., Cesari, D., Donateo, A., Chirizzi, D., and Belosi, F.: Characterization of PM10 and PM2.5 and Their Metals Content in Different Typologies of Sites in South-Eastern Italy, Atmosphere, 5, doi:10.3390/atmos5020435, 2014.

Dai, F., Chen, M., and Yang, B.: Spatiotemporal variations of PM2.5 concentration at the neighborhood level in five Chinese megacities, Atmospheric Pollution Research, 11, 190-202, https://doi.org/10.1016/j.apr.2020.03.010, 2020.

Fang, K., Wang, T., He, J., Wang, T., Xie, X., Tang, Y., Shen, Y., and Xu, A.: The distribution and drivers of PM2.5 in a rapidly urbanizing region: The Belt and Road Initiative in focus, Science of The Total Environment, 716, 137010, https://doi.org/10.1016/j.scitotenv.2020.137010, 2020.

Gao, J., Tian, H., Cheng, K., Lu, L., Zheng, M., Wang, S., Hao, J., Wang, K., Hua, S., Zhu, C., and Wang, Y.: The variation of chemical characteristics of PM2.5 and PM10 and formation causes during two haze pollution events in urban Beijing, China, Atmospheric Environment, 107, 1-8, https://doi.org/10.1016/j.atmosenv.2015.02.022, 2015.

Gebhart, K. A., Schichtel, B. A., Malm, W. C., Barna, M. G., Rodriguez, M. A., and Collett, J. L.: Back-trajectory-based source apportionment of airborne sulfur and nitrogen concentrations at Rocky Mountain National Park, Colorado, USA, Atmospheric Environment, 45, 621-633, https://doi.org/10.1016/j.atmosenv.2010.10.035, 2011.

Govender, P. and Sivakumar, V.: Application of k-means and hierarchical clustering techniques for analysis of air pollution: A review (1980–2019), Atmospheric Pollution Research, 11, 40-56, https://doi.org/10.1016/j.apr.2019.09.009, 2020.

Gurjar, B. R., Ravindra, K., and Nagpure, A. S.: Air pollution trends over Indian megacities and their local-to-global implications, Atmospheric Environment, 142, 475-495, https://doi.org/10.1016/j.atmosenv.2016.06.030, 2016.

https://doi.org/10.5194/acp-2021-311
Preprint. Discussion started: 9 June 2021

Han, Y.-J., Holsen, T. M., and Hopke, P. K.: Estimation of source locations of total gaseous mercury measured in New York State using trajectory-based models, Atmospheric Environment, 41, 6033-6047, https://doi.org/10.1016/j.atmosenv.2007.03.027, 2007.

Hasheminassab, S., Daher, N., Saffari, A., Wang, D., Ostro, B. D., and Sioutas, C.: Spatial and temporal variability of sources of ambient fine particulate matter (PM2.5) in California, Atmos. Chem. Phys., 14, 12085-12097, doi:10.5194/acp-14-12085-2014, 2014.

He, J., Ding, S., and Liu, D.: Exploring the spatiotemporal pattern of PM2.5 distribution and its determinants in Chinese cities based on a multilevel analysis approach, Science of The Total Environment, 659, 1513-1525, https://doi.org/10.1016/j.scitotenv.2018.12.402, 2019.

Jiang, S. Y. N., Yang, F., Chan, K. L., and Ning, Z.: Water solubility of metals in coarse PM and PM2.5 in typical urban environment in Hong Kong, Atmospheric Pollution Research, 5, 236-244, https://doi.org/10.5094/APR.2014.029, 2014.

Kelly, F. J. and Fussell, J. C.: Size, source and chemical composition as determinants of toxicity attributable to ambient particulate matter, Atmospheric Environment, 60, 504-526, https://doi.org/10.1016/j.atmosenv.2012.06.039, 2012.

Kulshrestha, A., Satsangi, P. G., Masih, J., and Taneja, A.: Metal concentration of PM2.5 and PM10 particles and seasonal variations in urban and rural environment of Agra, India, Science of The Total Environment, 407, 6196-6204, https://doi.org/10.1016/j.scitotenv.2009.08.050, 2009a.

Kulshrestha, U. C., Sunder Raman, R., Kulshrestha, M. J., Rao, T. N., and Hazarika, P. J.: Secondary aerosol formation and identification of regional source locations by PSCF analysis in the Indo-Gangetic region of India, Journal of Atmospheric Chemistry, 63, 33-47, doi:10.1007/s10874-010-9156-z, 2009b.

Lee, J. H. and Hopke, P. K.: Apportioning sources of PM2.5 in St. Louis, MO using speciation trends network data, Atmospheric Environment, 40, 360-377, https://doi.org/10.1016/j.atmosenv.2005.11.074, 2006.

Li, G., Fang, C., Wang, S., and Sun, S.: The Effect of Economic Growth, Urbanization, and Industrialization on Fine Particulate Matter (PM2.5) Concentrations in China, Environmental Science & Technology, 50, 11452-11459, doi:10.1021/acs.est.6b02562, 2016.

Lin, G., Fu, J., Jiang, D., Hu, W., Dong, D., Huang, Y., and Zhao, M.: Spatio-Temporal Variation of PM2.5 Concentrations and Their Relationship with Geographic and Socioeconomic Factors in China, International Journal of Environmental Research and Public Health, 11, doi:10.3390/ijerph110100173, 2014.

Liu, G.-R., Shi, G.-L., Tian, Y.-Z., Wang, Y.-N., Zhang, C.-Y., and Feng, Y.-C.: Physically constrained source apportionment (PCSA) for polycyclic aromatic hydrocarbon using the Multilinear Engine 2-species ratios (ME2-SR) method, Science of The Total Environment, 502, 16-21, https://doi.org/10.1016/j.scitotenv.2014.09.011, 2015.

Luo, K., Li, G., Fang, C., and Sun, S.: PM2.5 mitigation in China: Socioeconomic determinants of concentrations and differential control policies, Journal of Environmental Management, 213, 47-55, https://doi.org/10.1016/j.jenvman.2018.02.044, 2018.

Mirowsky, J., Hickey, C., Horton, L., Blaustein, M., Galdanes, K., Peltier, R. E., Chillrud, S., Chen, L. C., Ross, J., Nadas, A., Lippmann, M., and Gordon, T.: The effect of particle size, location and season on the toxicity of urban and rural particulate matter, Inhalation Toxicology, 25, 747-757, doi:10.3109/08958378.2013.846443, 2013.

Ostro, B., Lipsett, M., Reynolds, P., Goldberg, D., Hertz, A., Garcia, C., Henderson Katherine, D., and Bernstein, L.: Long-Term Exposure to Constituents of Fine Particulate Air Pollution and Mortality: Results from the California Teachers Study, Environmental Health Perspectives, 118, 363-369, doi:10.1289/ehp.0901181, 2010.

Paatero, P.: Least squares formulation of robust non-negative factor analysis, Chemometrics and Intelligent Laboratory Systems, 37, 23-35, https://doi.org/10.1016/S0169-7439(96)00044-5, 1997.

Paatero, P. and Tapper, U.: Positive matrix factorization: A non-negative factor model with optimal utilization of error estimates of data values, Environmetrics, 5, 111-126, https://doi.org/10.1002/env.3170050203, 1994.

Pant, P. and Harrison, R. M.: Critical review of receptor modelling for particulate matter: A case study of India, Atmospheric Environment, 49, 1-12, https://doi.org/10.1016/j.atmosenv.2011.11.060, 2012.

Philip, S., Martin, R. V., van Donkelaar, A., Lo, J. W.-H., Wang, Y., Chen, D., Zhang, L., Kasibhatla, P. S., Wang, S., Zhang, Q., Lu, Z., Streets, D. G., Bittman, S., and Macdonald, D. J.: Global Chemical Composition of Ambient Fine Particulate Matter for Exposure Assessment, Environmental Science & Technology, 48, 13060-13068, doi:10.1021/es502965b, 2014.

Polissar, A. V., Hopke, P. K., and Poirot, R. L.: Atmospheric Aerosol over Vermont: Chemical Composition and Sources, Environmental Science & Technology, 35, 4604-4621, doi:10.1021/es0105865, 2001.

Richard, A., Gianini, M. F. D., Mohr, C., Furger, M., Bukowiecki, N., Minguillón, M. C., Lienemann, P., Flechsig, U., Appel, K., DeCarlo, P. F., Heringa, M. F., Chirico, R., Baltensperger, U., and Prévôt, A. S. H.: Source apportionment of size and time resolved trace elements and organic aerosols from an urban courtyard site in Switzerland, Atmos. Chem. Phys., 11, 8945-8963, doi:10.5194/acp-11-8945-2011, 2011.

Riuttanen, L., Hulkkonen, M., Dal Maso, M., Junninen, H., and Kulmala, M.: Trajectory analysis of atmospheric transport of fine particles, SO2, NOx and O3 to the SMEAR II station in Finland in 1996–2008, Atmos. Chem. Phys., 13, 2153-2164, doi:10.5194/acp-13-2153-2013, 2013.

Saxena, A., Prasad, M., Gupta, A., Bharill, N., Patel, O. P., Tiwari, A., Er, M. J., Ding, W., and Lin, C.-T.: A review of clustering techniques and developments, Neurocomputing, 267, 664-681, https://doi.org/10.1016/j.neucom.2017.06.053, 2017.

Seto, K. C., Golden, J. S., Alberti, M., and Turner, B. L.: Sustainability in an urbanizing planet, Proceedings of the National Academy of Sciences, 114, 8935, doi:10.1073/pnas.1606037114, 2017.

Shi, G.-L., Feng, Y.-C., Zeng, F., Li, X., Zhang, Y.-F., Wang, Y.-Q., and Zhu, T.: Use of a Nonnegative Constrained Principal Component Regression Chemical Mass Balance Model to Study the Contributions of Nearly Collinear Sources, Environmental Science & Technology, 43, 8867-8873, doi:10.1021/es902785c, 2009.

Tian, Y.-Z., Chen, G., Wang, H.-T., Huang-Fu, Y.-Q., Shi, G.-L., Han, B., and Feng, Y.-C.: Source regional contributions to PM2.5 in a megacity in China using an advanced source regional apportionment method, Chemosphere, 147, 256-263, https://doi.org/10.1016/j.chemosphere.2015.12.132, 2016.

Tian, Y. Z., Wang, J., Peng, X., Shi, G. L., and Feng, Y. C.: Estimation of the direct and indirect impacts of fireworks on the physicochemical characteristics of atmospheric PM10 and PM2.5, Atmos. Chem. Phys., 14, 9469-9479, doi:10.5194/acp-14-9469-2014, 2014.

Timmermans, R., Kranenburg, R., Manders, A., Hendriks, C., Segers, A., Dammers, E., Zhang, Q., Wang, L., Liu, Z., Zeng, L., Denier van der Gon, H., and Schaap, M.: Source apportionment of PM2.5 across China using LOTOS-EUROS, Atmospheric Environment, 164, 370-386, https://doi.org/10.1016/j.atmosenv.2017.06.003, 2017.

Vassura, I., Venturini, E., Marchetti, S., Piazzalunga, A., Bernardi, E., Fermo, P., and Passarini, F.: Markers and influence of open biomass burning on atmospheric particulate size and composition during a major bonfire event, Atmospheric Environment, 82, 218-225, https://doi.org/10.1016/j.atmosenv.2013.10.037, 2014.

Wang, N., Zhu, H., Guo, Y., and Peng, C.: The heterogeneous effect of democracy, political globalization, and urbanization on PM2.5 concentrations in G20 countries: Evidence from panel quantile regression, Journal of Cleaner Production, 194, 54-68, https://doi.org/10.1016/j.jclepro.2018.05.092, 2018a.

Wang, Q., Fang, J., Shi, W., and Dong, X.: Distribution characteristics and policy-related improvements of PM2.5 and its components in six Chinese cities, Environmental Pollution, 266, 115299, https://doi.org/10.1016/j.envpol.2020.115299, 2020.

Wang, Z., Zheng, F., Zhang, W., and Wang, S.: Analysis of SO2 Pollution Changes of Beijing-Tianjin-Hebei Region over China Based on OMI Observations from 2006 to 2017, Advances in Meteorology, 2018, 8746068, doi:10.1155/2018/8746068, 2018b.

https://doi.org/10.5194/acp-2021-311
Preprint. Discussion started: 9 June 2021

Atmospheric Chemistry and Physics Discussions

Wu, J., Bei, N., Wang, Y., Li, X., Liu, S., Liu, L., Wang, R., Yu, J., Le, T., Zuo, M., Shen, Z., Cao, J., Tie, X., and Li, G.: Insights into particulate matter pollution in the North China Plain during wintertime: local contribution or regional transport?, Atmos. Chem. Phys., 21, 2229-2249, doi:10.5194/acp-21-2229-2021, 2021.

Xu, G., Ren, X., Xiong, K., Li, L., Bi, X., and Wu, Q.: Analysis of the driving factors of PM2.5 concentration in the air: A case study of the Yangtze River Delta, China, Ecological Indicators, 110, 105889, https://doi.org/10.1016/j.ecolind.2019.105889, 2020a.

Xu, J., Shi, J., Zhang, Q., Ge, X., Canonaco, F., Prévôt, A. S. H., Vonwiller, M., Szidat, S., Ge, J., Ma, J., An, Y., Kang, S., and Qin, D.: Wintertime organic and inorganic aerosols in Lanzhou, China: sources, processes, and comparison with the results during summer, Atmos. Chem. Phys., 16, 14937-14957, doi:10.5194/acp-16-14937-2016, 2016.

Xu, Q., Zhang, Q., Liu, J., and Luo, B.: Efficient synthetical clustering validity indexes for hierarchical clustering, Expert Systems with Applications, 151, 113367, https://doi.org/10.1016/j.eswa.2020.113367, 2020b.

Yan, D., Lei, Y., Shi, Y., Zhu, Q., Li, L., and Zhang, Z.: Evolution of the spatiotemporal pattern of PM2.5 concentrations in China – A case study from the Beijing-Tianjin-Hebei region, Atmospheric Environment, 183, 225-233, https://doi.org/10.1016/j.atmosenv.2018.03.041, 2018.

Yang, D., Chen, Y., Miao, C., and Liu, D.: Spatiotemporal variation of PM2.5 concentrations and its relationship to urbanization in the Yangtze river delta region, China, Atmospheric Pollution Research, 11, 491-498, https://doi.org/10.1016/j.apr.2019.11.021, 2020.

Yang, D., Ye, C., Wang, X., Lu, D., Xu, J., and Yang, H.: Global distribution and evolvement of urbanization and PM2.5 (1998–2015), Atmospheric Environment, 182, 171-178, https://doi.org/10.1016/j.atmosenv.2018.03.053, 2018a.

Yang, Y., Pun, V. C., Sun, S., Lin, H., Mason, T. G., and Qiu, H.: Particulate matter components and health: a literature review on exposure assessment, Journal of Public Health and Emergency, 2, doi:10.21037/jphe.2018.03.03, 2018b.

Zhang, R., Wang, G., Guo, S., Zamora, M. L., Ying, Q., Lin, Y., Wang, W., Hu, M., and Wang, Y.: Formation of Urban Fine Particulate Matter, Chemical Reviews, 115, 3803-3855, doi:10.1021/acs.chemrev.5b00067, 2015.

Zhang, R., Jing, J., Tao, J., Hsu, S. C., Wang, G., Cao, J., Lee, C. S. L., Zhu, L., Chen, Z., Zhao, Y., and Shen, Z.: Chemical characterization and source apportionment of PM2.5 in Beijing: seasonal perspective, Atmos. Chem. Phys., 13, 7053-7074, doi:10.5194/acp-13-7053-2013, 2013.

Zhang, Y., Shuai, C., Bian, J., Chen, X., Wu, Y., and Shen, L.: Socioeconomic factors of PM2.5 concentrations in 152 Chinese cities: Decomposition analysis using LMDI, Journal of Cleaner Production, 218, 96-107, https://doi.org/10.1016/j.jclepro.2019.01.322, 2019.

Zhao, B., Wang, S., Wang, J., Fu, J. S., Liu, T., Xu, J., Fu, X., and Hao, J.: Impact of national NOx and SO2 control policies on particulate matter pollution in China, Atmospheric Environment, 77, 453-463, https://doi.org/10.1016/j.atmosenv.2013.05.012, 2013.

https://doi.org/10.5194/acp-2021-311
Preprint. Discussion started: 9 June 2021

Atmospheric Chemistry and Physics Discussions

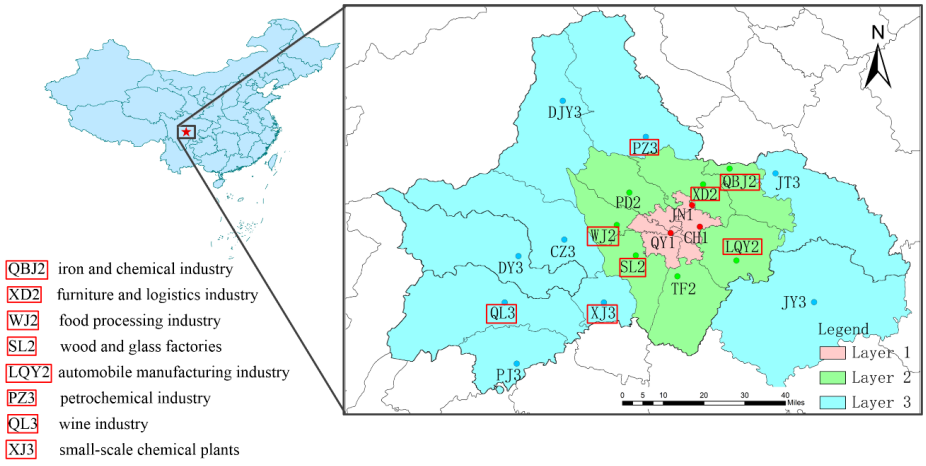

565 **Figure 1: The locations of 19 sampling sites in Chengdu from 2015 to 2019. Sampling sites marked with red box were characterized by various industries as descried in the left part of the figure. More details of sampling sites were listed in Table S1.**

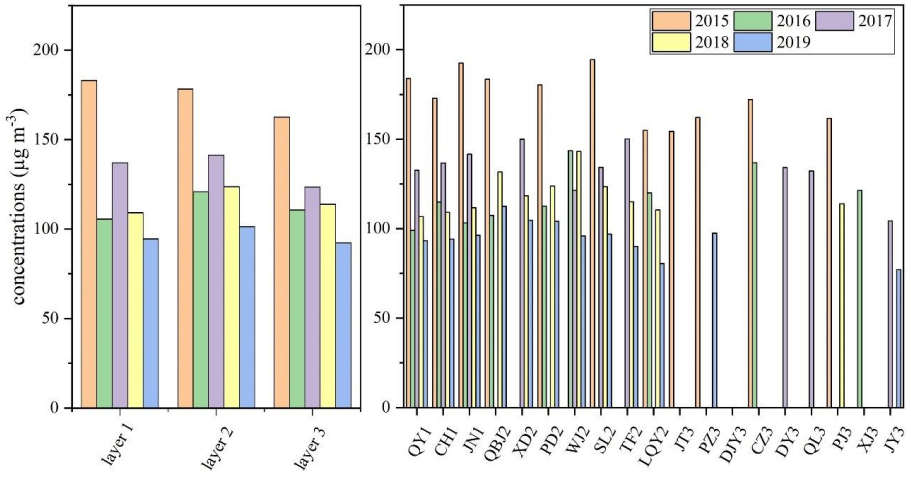

Figure 2. Spatiotemporal variations of $PM_{2.5}$ concentrations for layers and sampling sites in 2015-2019.

https://doi.org/10.5194/acp-2021-311
Preprint. Discussion started: 9 June 2021

Atmospheric Chemistry and Physics Discussions

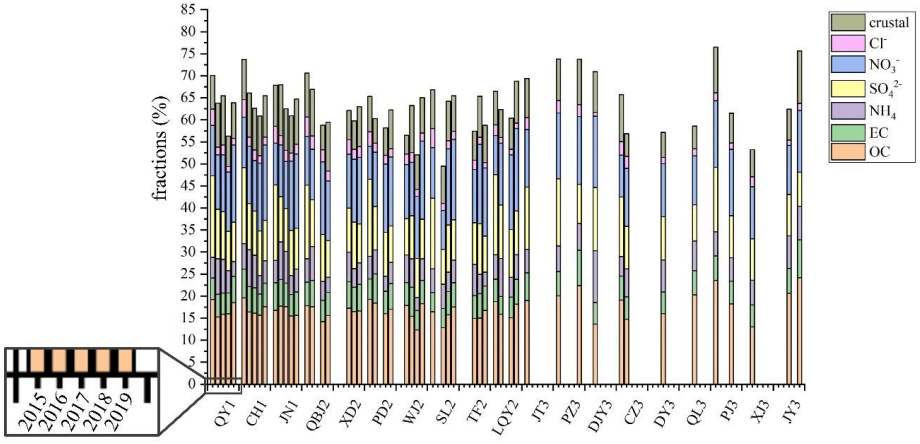

570 **Figure 3. The spatiotemporal variations of the fractions of main chemical species in $PM_{2.5}$ at each site during winters in 2015 to 2019. Unit: %**

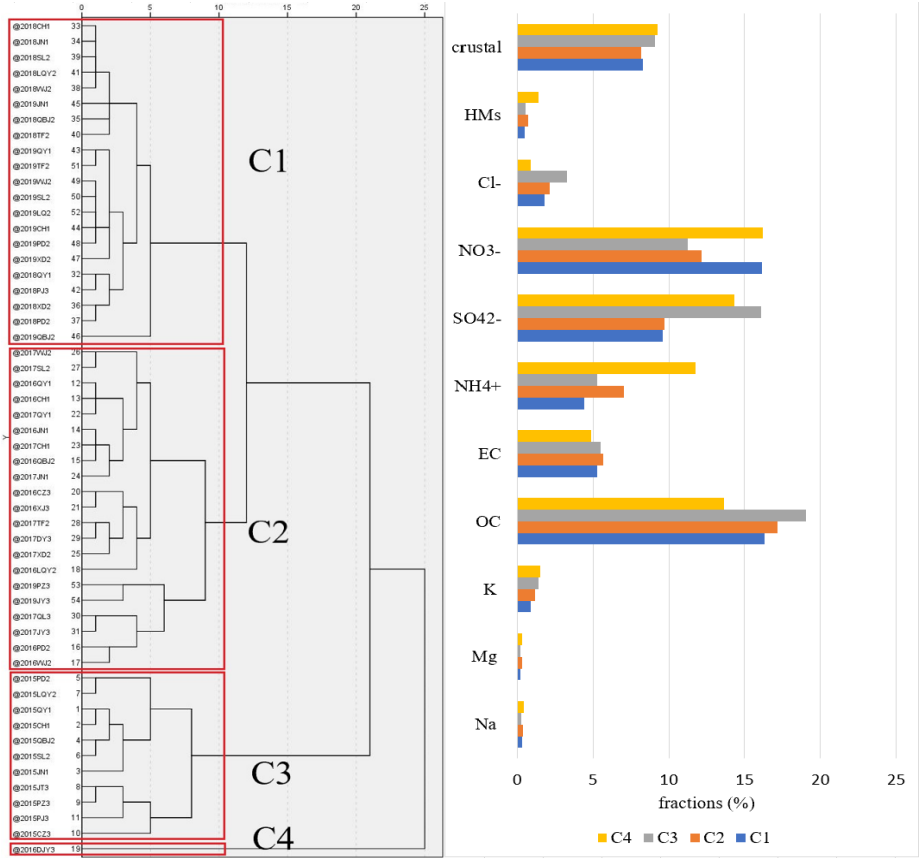

575 **Figure 4. The HCA results (based on cosine distances) of chemical species (%) at sampling sites for five years (2015-2019) and their averaged species fractions.**

https://doi.org/10.5194/acp-2021-311
Preprint. Discussion started: 9 June 2021

Atmospheric Chemistry and Physics Discussions

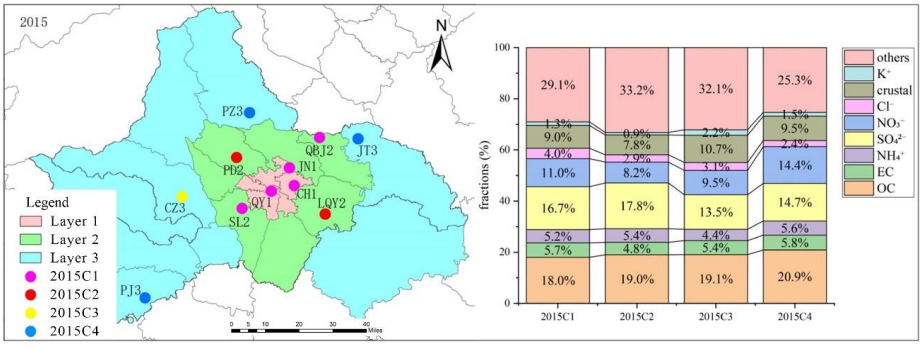

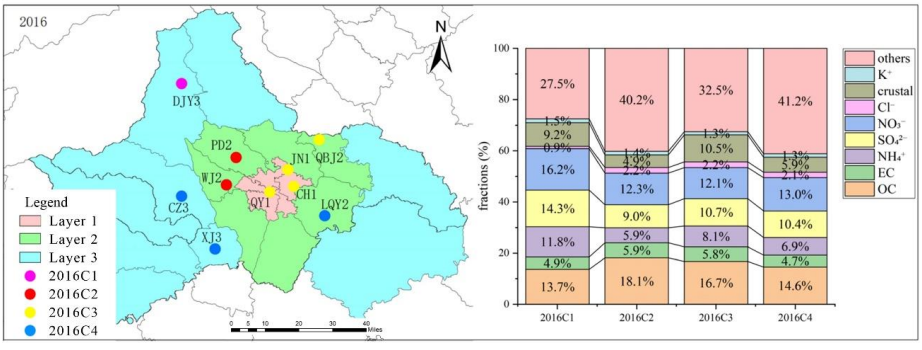

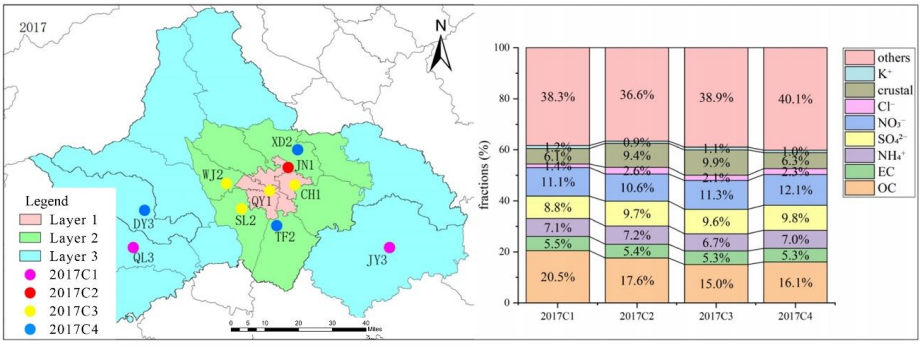

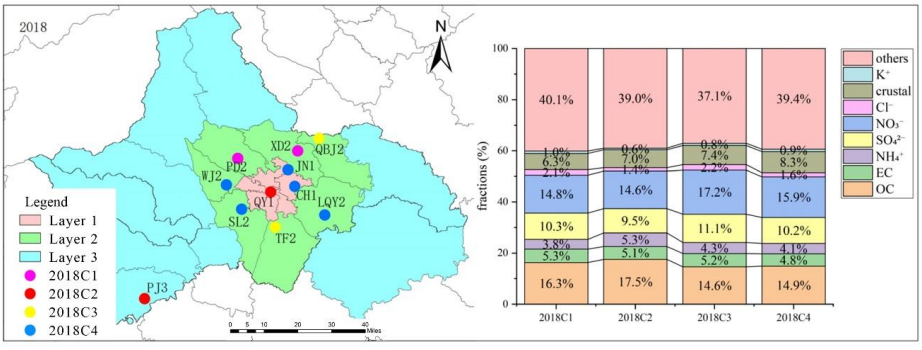

580

https://doi.org/10.5194/acp-2021-311
Preprint. Discussion started: 9 June 2021

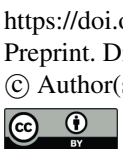

Atmospheric Chemistry and Physics Discussions

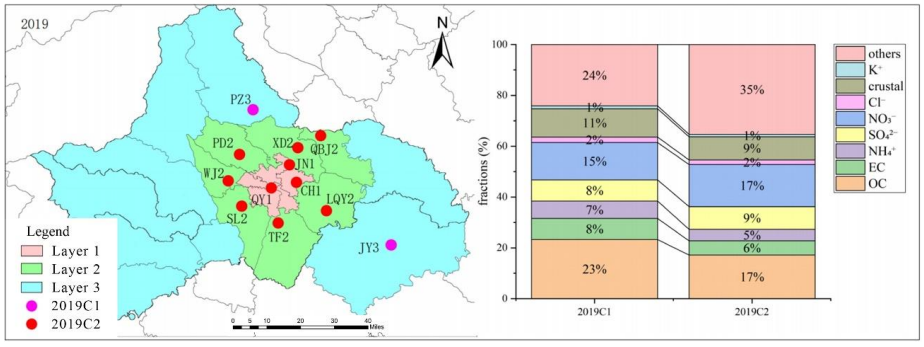

Figure 5. Spatial distribution of $PM_{2.5}$ compositions and fraction values of each cluster from 2015 to 2019. (i.e. 2015C1 refers to the first cluster of sampling sites in 2015).

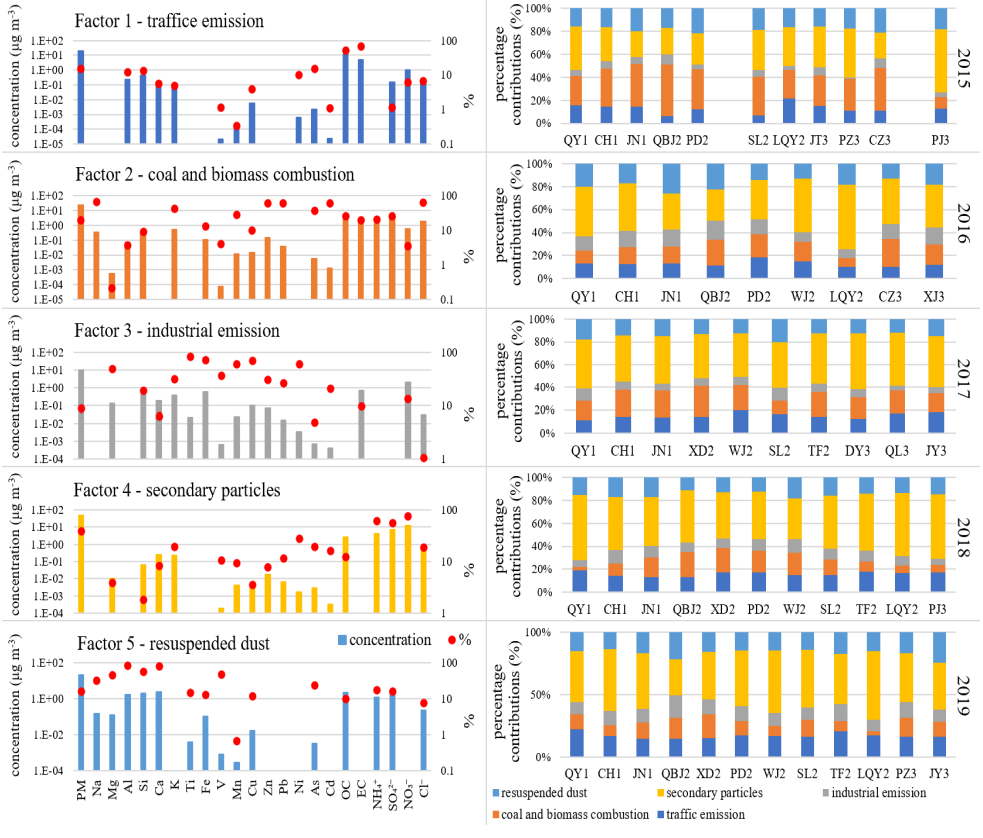

585 **Figure 6. Source profiles estimated by the PMF, in the form of species concentrations (μg.m^{-3}) and percentages of species sum (%).**

https://doi.org/10.5194/acp-2021-311
Preprint. Discussion started: 9 June 2021

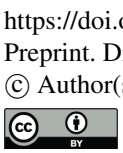

Atmospheric Chemistry and Physics Discussions

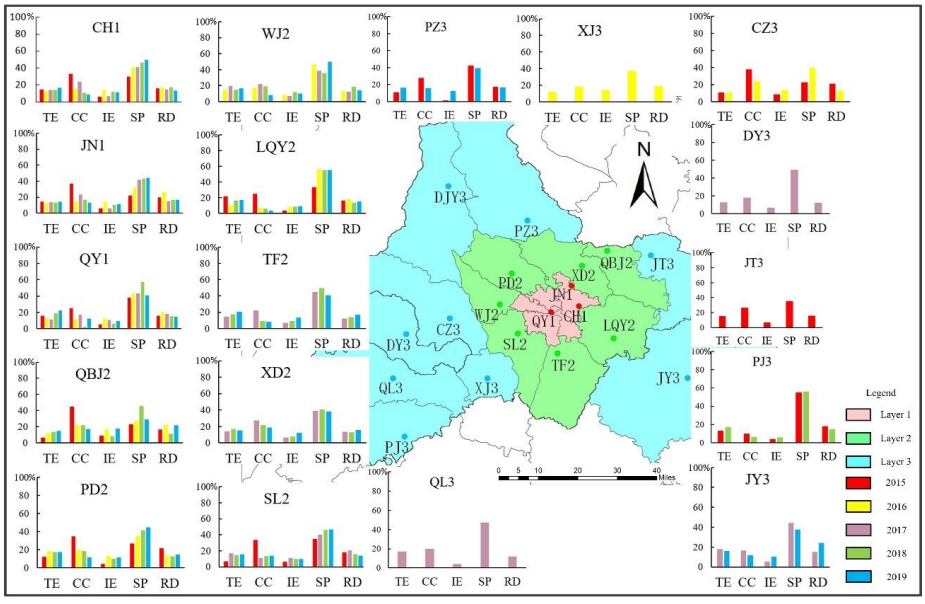

Figure 7. Spatiotemporal variations of source contributions to total mass of $PM_{2.5}$ in Chengdu. (TE, CC, IE, SP and RD represent traffic emission, coal and biomass combustion, industrial emission, secondary particles and resuspended dust, respectively.)

590

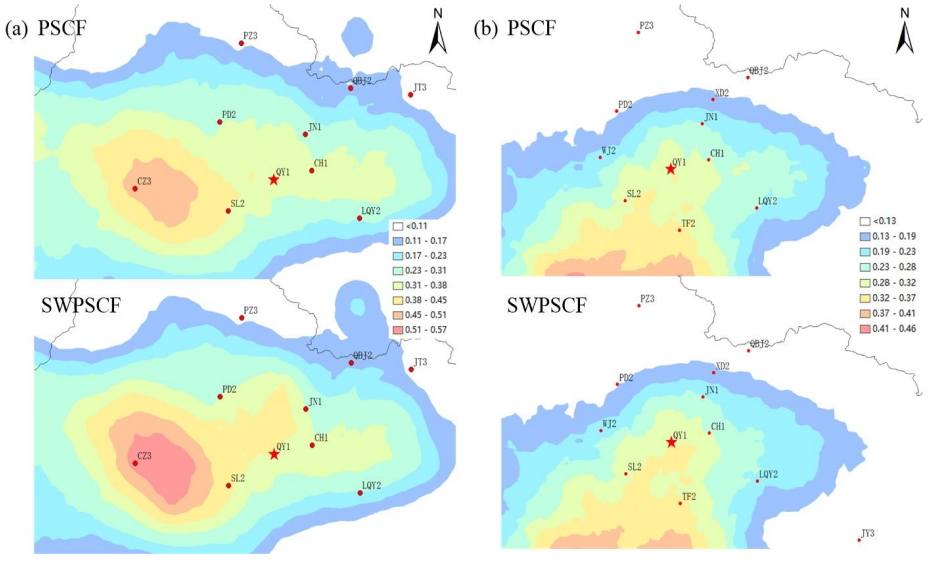

Figure 8. Potential source locations identified by the PSCF and SWPSCF method: (a) coal and biomass combustion source in 2015; (b) traffic emission source in 2019.